Pharm Res (2015) 32:723–735
DOI 10.1007/s11095-014-1504-2

RESEARCH PAPER

Methoxy Poly(ethylene glycol)-Poly(lactide) Nanoparticles Encapsulating Quercetin Act as an Effective Anticancer Agent by Inducing Apoptosis in Breast Cancer

Garima Sharma • Jongbong Park • Ashish Ranjan Sharma • Jun-Sub Jung • Haesung Kim • Chiranjib Chakraborty • Dong-Keun Song • Sang-Soo Lee • Ju-Suk Nam

Received: 4 February 2014 / Accepted: 22 August 2014 / Published online: 4 September 2014

ABSTRACT

Purpose To overcome the therapeutic restrictions offered by hydrophobic quercetin (Qu), this study aims to synthesize MPEG-PLA encapsulated Qu nanoparticle and to evaluate their anticancer efficacy.

Materials and Methods *In vitro* anticancer potential and apoptotic studies were done by cell cytotoxicity assay and flow cytometry, respectively. MPEG-PLA-Qu nanoparticles were evaluated for anticancer efficacy *in vivo* using xenograft mice model. TUNEL assay was performed to observe the frequency of apoptotic cells *in vivo*.

Results The hydrodynamic particle size, polydispersity index, zeta potential and drug loading % of MPEG-PLA-Qu nanoparticle was 155.3 ± 3.2 nm, 0.2 ± 0.05, −3.14 mV and 5.3 ± 1.1%, respectively. Also, MPEG-PLA-Qu showed sustained drug release for 10 days. *In vitro* results showed that MPEG-PLA-Qu could efficiently induce apoptosis in triple negative breast cancer cell line (MDA-MB-231) with higher amount of quercetin in cell lysate treated with MPEG-PLA-Qu in comparison to free quercetin. In xenograft model for breast cancer, peritumorally injected MPEG-PLA-Qu significantly inhibited the tumor growth. Moreover, TUNEL assay showed more occurrence of apoptotic cells in MPEG-PLA-Qu treated tumors compared to free quercetin at similar dose.

Conclusion Our data suggest that MPEG-PLA-Qu nanoparticle can have a promising clinical potential for the treatment of breast cancer.

KEY WORDS apoptosis · breast cancer · MPEG-PLA · nanoparticle · quercetin

ABBREVATIONS

DL	Drug loading
EE	Encapsulation efficiency
ELS	Electrophoretic light scattering spectrophotometer
MPEG-PLA	Methoxy poly(ethylene glycol)-poly(lactide)
Qu	Quercetin
TEM	Transmission electron microscope

INTRODUCTION

Breast cancer is among the second most commonly occurred cancer worldwide. According to World Health Organization,

Garima Sharma and Jongbong Park contributed equally to this work.

Electronic supplementary material The online version of this article (doi:10.1007/s11095-014-1504-2) contains supplementary material, which is available to authorized users.

G. Sharma • J. Park • A. Sharma • H. Kim • C. Chakraborty • S.-S. Lee • J.-S. Nam
Institute for Skeletal Aging & Orthopaedic Surgery, Hallym University-Chuncheon Sacred Heart Hospital Chuncheon, Republic of Korea

J.-S. Jung • D.-K. Song
Department of Pharmacology, Institute of Natural Medicine, College of Medicine, Hallym University Chuncheon, Republic of Korea

G. Sharma
Amity Institute of Nanotechnology, Amity University Uttar Pradesh Noida, Uttar Pradesh, India

C. Chakraborty
Department of Bioinformatics, School of Computer Sciences, Galgotias University Greater Noida, India

S.-S. Lee (✉) • J.-S. Nam (✉)
Institute for Skeletal Aging, College of Medicine 6th 3607, Hallym University 1 Hallymdaehakgil, Chuncheon, Gangwon-do 200-702 Republic of Korea
e-mail: totalhip@hallym.ac.kr
e-mail: jsnam88@hallym.ac.kr

approximately 1.6 million new cases of breast cancer were reported in 2012 while mortality cases from breast cancer reached to 522,000 in 2012 [1]. In the present scenario of increasing breast cancer incidence throughout the world among women, new chemopreventive formulations are in constant demand to reduce the side effects of conventional therapies like surgery, chemotherapy, radiotherapy, hormone therapy and targeted therapy. Natural compounds present in plants serve as a better choice to be explored as an effective anticancer agents. Quercetin (3,5,7,3′,4′-pentahydroxy flavone) is among such naturally occurring compounds, widely present in leaves, vegetables, fruits and grains [2]. Owing to the high number of hydroxyl groups and conjugated π orbitals, quercetin is considered as a potent free-radical scavenging antioxidant compound [3]. In addition, quercetin has also been reported to be effective in inflammation, arteriosclerosis, bleeding, allergy and swellings [4]. Nowadays, quercetin has received increasing attention as a pro-apoptotic flavonoid with antiproliferative effect on tumor cells rather than normal or non-transformed cells [5]. As reported earlier, quercetin inhibits cell proliferation by modulating signaling pathways leading to cell apoptosis [6]. Despite of the promising application of quercetin as a chemopreventive agent, its clinical use is restricted because of its hydrophobicity [7]. Previous studies also reported short half life span of quercetin in body fluids [8]. These limitations can be overcome by encapsulating quercetin into biodegradable polymer, making the drug completely dispersible in water.

In the past few decades, various biodegradable polymers have been used to encapsulate hydrophobic anticancer drugs to increase their water solubility, antitumor efficacy, tumor targeting, drug delivery and controlled release [9]. Some biodegradable polymer encapsulated anticancer drugs are already in clinical trial phases or marketed. Polylactic acid (PLA) is a synthetic biodegradable polymer approved by the US Food and Drug Administration and is widely studied to encapsulate hydrophobic anticancer drugs [10]. It hydrolyzes into nontoxic hydroxyl-carboxylic acid through ester bond cleavage and enters into citric acid cycle, finally metabolizing into water and carbon dioxide. Preparation of quercetin encapsulated PLA nanoparticles has been previously suggested [11]. Regardless of its various advantages, PLA nanoparticles are rapidly cleared off from circulatory system after systemic injection, thus reducing the expected effect of the drug [12]. It has been earlier reported that the elimination of PLA encapsulated drug from blood stream by reticulo-endothelial system (RES) can be avoided by surface modification of the nanoparticles. It is well established that copolymerization of PLA with polyethylene glycol (PEG) can improve hydrophilicity, flexibility, antiphagocytosis against macrophages, resistance to immunological recognition, non-combination with proteins, and biocompatibility to nanoparticle [13]. Additionally, PEGylation of PLA polymer can shift the negative surface charge of nanoparticles towards neutral charge, facilitating the interaction of polymeric nanoparticles with cell membrane and internalization of drug loaded nanoparticles by tumor cells more efficiently [14]. The difference in the biodistribution and uptake of PEG coated nanoparticles is due to steric repulsion forces which prevents adsorption of phagocytic cells specific opsonin proteins leading to delay in opsonization mechanism [15]. Thus, to achieve better therapeutic effects on breast cancer, PEG-PLA encapsulated quercetin nanoparticles can be a suitable drug delivery system.

Moreover, other problems associated with chemopreventive agents include poor targeting and low concentration in the tumor can be eliminated by peritumoral injection of drug at the local site of tumor [16]. Earlier reports suggested increased drug concentration in peritumoral region and lymph nodes after peritumoral injection of drug adsorbed onto activated carbon particles for loco-regional chemotherapy for breast cancer [17]. This approach was considered effective for tumors sites which are easily accessible. Furthermore, locally injected nanoparticles were found to be gradually adsorbed into the lymphatic system by infiltrating into the interstitial spaces surrounding tumor. Thus, local injection of drug loaded nanoparticles into peritumoral region can be used as a tool for lymphatic targeting and preventing metastases. Recent studies explored the anticancer potential of polymer encapsulated quercetin against various cancer cell lines, *e.g.* ovarian cancer [18] and lung cancer, the efficacy of quercetin encapsulated in polymeric nanoparticulate systems in inhibiting breast cancer is rarely studied. Thus, it is interesting to explore the anticancer effect of polymer encapsulated quercetin which is injected peritumorally on breast cancer.

In this study, MPEG-PLA encapsulated quercetin nanoparticles were synthesized to develop a novel drug delivery system. Further, this study aims at evaluating the anticancer efficiency and induction of cell apoptosis by peritumorally administered MPEG-PLA-Qu nanoparticles against breast cancer cells in detail.

MATERIALS AND METHODS

Preparation of MPEG-PLA-Qu Nanoparticles

MPEG-PLA block copolymer (polylactide average M_n ~5,000, PEG average M_n ~5,000: Sigma-Aldrich, St. Louis, MO, USA) was used as a copolymer to encapsulated quercetin (Sigma-Aldrich). MPEG-PLA-Qu nanoparticles were synthesized by previously reported nanoprecipitation with slight modifications [19]. For nanoprecipitation method ten mg of MPEG-PLA and 0.5 mg of quercetin were dissolved in 1 ml acetonitrile. The above organic solvent was added drop wise into aqueous solution of 0.25% Pluronic F-68 (Sigma-Aldrich) and stirred for 1 h. The nanoparticle dispersion was further

stirred for 3–4 h to evaporate the remaining organic solvent. MPEG-PLA-Qu nanoparticles were recovered by centrifugation (15,000 rpm for 1 h) and washed twice with distilled water to remove free drug and were lyophilized. The preparation of empty MPEG-PLA nanoparticles was same as mentioned above without quercetin in the mixture. For cellular uptake studies, MPEG-PLA-Qu nanoparticles co-encapsulating Nile Red (Sigma-Aldrich) was synthesized by adding 10 μg Nile red along with quercetin to 10 mg of MPEG-PLA copolymer and following similar method afterwards.

Particle Size and Zeta Potential Analysis

Particle sizes and distribution pattern were determined by commercially available electrophoretic light scattering spectrophotometer (Photal ELS-8000, Otsuka Electronics, Japan) with 90° scattering angle at 25°C. ELS-8000 was also used to determine the zeta potential of MPEG-PLA-Qu nanoparticles by measuring their electrophoretic mobility. Before measurement, 1 mg of MPEG-PLA-Qu nanoparticles was appropriately diluted in distilled water and KCl (1 mM) for zeta size analysis and zeta potential analysis, respectively. Analysis was performed twice for accuracy.

Surface Morphology Analysis

Transmission electron microscope (TEM; JEM-2010, JEOL, Japan) at accelerating voltage of 0–120 kV was used to analyze the shape and morphology of MPEG-PLA-Qu nanoparticles. TEM samples were prepared by mechanically transferring MPEG-PLA-Qu nanoparticles on a 200 mesh carbon coated copper TEM grid and further negatively stained by 1% alkaline phosphotungstic acid for 1 min.

To observe the surface morphology of MPEG-PLA-Qu nanoparticles, atomic force microscopy (AFM; Bruker Multimode 8) was also performed with Nanoscope V controller (Bruker AXS Inc., Madison, WI, USA). For analysis, a drop of nanoparticle suspension was deposited and air dried on silicon surface. Images were obtained by AFM on tapping mode using probe tip radius≤8 nm with spring constant of 40 N/m and scan rate of 1 Hz.

Drug Loading and Encapsulation Efficiency Analysis

Drug loading (DL) and encapsulation efficiency (EE) of MPEG-PLA-Qu nanoparticles were estimated using well accepted UV-visible spectrophotometric analysis with slight modification [20]. In brief, to determine DL and EE, ten mg of lyophilized MPEG-PLA-Qu nanoparticles were dissolved in 0.1 ml acetonitrile and quantified for quercetin content in UV-visible spectrophotometer at 380 nm (SpectraMax M2e, California) using standard curve prepared by known amounts of quercetin. DL was calculated as percent ratio of amount of quercetin in nanoparticles to the amount of nanoparticle (eq. 1) and EE was calculated as percent ratio of amount of quercetin in nanoparticles to the total amount of quercetin feeded in the formulation (eq. 2) [21].

$$DL(\%) = \frac{amount\ of\ drug\ in\ np}{total\ amount\ of\ np} \times 100 \quad (1)$$

$$EE(\%) = \frac{amount\ of\ drug\ in\ np}{total\ amount\ of\ feeding\ drug} \times 100 \quad (2)$$

In Vitro Drug Release Assay

In vitro quercetin-release from MPEG-PLA-Qu nanoparticles was studied at pH 7.4 with a modified dialysis method. 15 mg nanoparticles were resuspended in 2 ml phosphate buffer saline (PBS; pH 7.4) and then transferred into dialysis tubes (MWCO 8–10 KD). Dialysis tubes were placed in their respective buffered solution (1,000 ml) with constant stirring at 37°C. At each selected time interval (0, 6, 12, 24, 48, 72, 120, 168, 216 h) samples were withdrawn from dialysis tubes. Afterwards, acetonitrile was added to aliquoted samples in 1:1 ratio and mixed vigorously. Remaining quercetin in nanoparticles was determined by absorbance assay at 380 nm. The percent drug release was calculated using quercetin mass (M), measured at t=0 min and predetermined time points (t=n) and plotted against time (eq. 3). During the release assay the sink condition was maintained by changing buffered solutions after every 6 h.

$$Quercetin\ release(t = n, \%) = \frac{M(t = 0) - M(t = n)}{M(t = 0)} \times 100 \quad (3)$$

Cell Culture

Murine mammary cancer cell line, 4 T1 (ATCC, CRL-2539) was cultured in RPMI 1640 medium (Invitrogen, Carlsbad, CA) and human breast cancer cell line MDA-MB-231(ATCC HTB-26) in DMEM (Corning, USA) medium, supplemented with 10% fetal bovine serum (FBS), 100 U/ml penicillin, and 100 U/ml streptomycin (Lonza, Basel, Switzerland). Cells were cultured at 37°C in a humidified atmosphere of 5% CO_2, till it reached a confluence of 70 to 80%.

Cell Viability Assay

MDA-MB-231 cells were cultured in 96-well plates at a concentration of 2×10^4 cells/well for 24 h. Cells were then treated with vehicle (0.16% DMSO), free quercetin

(13.5 μg/ml; 40 μM) or MPEG-PLA-Qu nanoparticles at concentrations equivalent to 3.375, 6.75 and 13.5 μg/ml of loaded quercetin (in accordance with drug loading percent) at 37°C in 5% CO_2 for 96 h. Empty MPEG-PLA nanoparticles equal to the amount of MPEG-PLA-Qu nanoparticles (13.5 μg/ml dose) was used as control to observe the cytotoxic effect of polymer. Ten micro liters of 3-(4,5-dimethlthiazol-2-yl)-2,5-diphenyl-tetrazoliumbromide (MTT) (5 mg/ml dissolved in PBS; Sigma, St. Lois, MO, USA) was added to each well, and the plates were incubated at 37°C for 2 h. The supernatant was discarded and 200 μl of dimethyl sulfoxide (DMSO; Sigma) was added to dissolve the blue insoluble MTT formazan produced bymitochondrial succinate dehydrogenase. The optical density was measured at wavelength of 570 nm. Experiments were repeated three times and the data were expressed as the means ± SD.

Lactate Dehydrogenase (LDH) Activity Assay

The cytotoxic effect of MPEG-PLA-Qu nanoparticles was determined using cytotoxicity detection kit (Takara Bio Inc., Shiga, Japan) according to manufacturer's protocol. In brief, cells were seeded on 96-well plates for 24 h for stabilization followed by treatment, as described in MTT assay section. After 96 h of treatment, cell culture medium (10 μl) was collected from each experimental set and mixed with PBS (40 μl) in a 96 well plate. Thereafter, 50 μl of LDH reagent was added to each well and incubated for 45 min at 25°C, in dark. The enzymatic reaction was stopped by adding 50 μl of stop solution and optical density was measured at 490 nm. Total cell lysate was used as positive control for cell death.

Assessment of Cell Apoptosis

To analyze early and late apoptotic changes in MDA-MB-231 cells, Annexin V-FITC/PI double staining assay kit (BD Pharmingen, San Diego, CA) was utilized. Cells were treated with MPEG-PLA-Qu (3.375, 6.75 and 13.5 μg/ml of loaded quercetin) for 72 h. Afterwards, Cells ($\sim 1\times10^6$) were collected, washed twice with PBS and suspended in 400 μl of binding buffer (added with 5 μl of annexin V-FITC and 5 μl of PI) for quantification of vital, apoptotic and necrotic cells. Annexin V binds to phosphatidylserine located on the outer surface of apoptotic cells. Thus, annexin V staining provides direct apoptotic cell count. After incubating the samples in the dark for 15 min at room temperature, the number of annexin V-FITC-positive and PI-positive cells in each field was determined by counting the cells directly on the flow cytometer (BD FACS Calibur).

Quantitative Estimation of Quercetin in Cell Lysate

Quantitative estimation of localized quercetin in MDA-MB-231 cells was carried out using spectrophotometry [22]. In brief, cells (1×10^6/well) were treated with quercetin (13.5 μg/ml) and MPEG-PLA-Qu nanoparticles (3.375, 6.75 and 13.5 μg/ml of loaded quercetin) for 72 h. Further, cells were washed twice with PBS and lysed in radioimmunoprecipitation assay buffer (RIPA; 20 mM Tris–HCl, pH 7.5, 200 mM NaCl, 1% Triton X-100, 1 mM dithiothreitol; T&I, Korea). The whole cell lysate was centrifuged at 12,000 rpm for 20 min and extracted with ethanol by vortexing to solubilize the quercetin in ethanol fraction. The absorption spectra of quercetin containing ethanol fraction was recorded at 380 nm using UV–vis spectrophotometer and the amount of quercetin was calculated using standard curve. To normalize, protein assay kit (Bio-Rad, Hercules, CA) was used to assay the protein concentration of total cell lysate.

Intracellular Uptake and Localization of Nanoparticles

After overnight incubation of MDA-MB-231 cells, seeded on 24 well plate under standard conditions, cells were treated with free Nile Red (0.3 μg) or MPEG-PLA nanoparticles coencapsulating quercetin and equal amount of Nile Red (MPEG-PLA-Qu-NR). At predetermined time points (1, 3, 6 and 72 h) cells were fixed and stained with ER tracker™ (Invitrogen) and 4 ,6-diamidino-2-phenylindole (DAPI; KPL, Gaithersburg, MD, USA) according to manufacturer's protocol. Cells were imaged under confocal microscope (Carl Zeiss LSM710, Germany) to determine the intracellular uptake and co-localization of MPEG-PLA nanoparticles with ER.

Xenograft Model for Breast Cancer

Breast cancer xenograft mouse models were developed as described previously [23]. All experiments with mice were performed according to guidelines and by approval of Animal Experimentation Ethics Committee at Hallym University, South Korea (Permit Number; 2009–41). The animals were acclimatized for 1 week before use and maintained throughout at standard conditions: 24±2°C temperature, 50±10% relative humidity, and 12-h light/12-h dark cycle. To establish tumor xenografts, 1×10^5 4 T1 cancer cells (suspended in DMEM without additives) were injected subcutaneously in the right flank of 5–6 weeks old female BALB/c mice (SAMTACO, Osan, Korea). Treatment started on day 10 (post inoculation) when tumors reached mean tumor volume of 100–200 mm^3. Mice were first randomized in 5 groups (n= 7) and were given peritumoral injection of saline, blank MPEG-PLA nanoparticles, free quercetin (4 mg/kg) and MPEG-PLA-Qu nanoparticles (equivalent to 0.5 and 4 mg/kg of loaded quercetin) dissolved in saline and thereafter

every 3rd day till day 19. Tumor size of each mouse was measured every 3rd day regularly till day 22 using vernier caliper and final tumor volume (V) was calculated using the formula $V = (l \times b^2)/2$, where l is the maximum diameter (mm) and b is the orthogonal diameter to l (mm). All mice were sacrificed at day 22 to remove tumors. Finally, tumors were weighed to determine and compare the anticancer efficiency of all the treatment groups. The body weight of mice was also monitored throughout the study to assess the possible treatment toxicity.

Pharmacokinetic Studies

In order to evaluate the pharmacokinetics of peritumorally administered MPEG-PLA-Qu nanoparticles, female BABL/c mice were inoculated with 4 T1 cells. On day 11th, single peritumoral injection of free quercetin and MPEG-PLA-Qu nanoparticles at a dose of 4 mg/kg were given. Later on, at defined time points (0, 12, 24 and 72 h) blood samples of five mice from each treatment groups were collected from their orbital cavity vein plexus, heparinized, and centrifuged at 2,500 rpm for 10 min at 4°C to obtain the plasma. Further, tumor tissues were excised and homogenized in RIPA buffer. Plasma samples and tissue homogenates were spiked with kaempferol (Sigma) as an experimental standard and acidified with 0.583 mol/l acetic acid. β-Glucuronidase (4 U/μl; Sigma) was further added into 0.1 ml plasma and 0.5 ml tissue samples to break the conjugation of quercetin with glucuronide and incubated in 37°C for 2 h. Plasma and the homogenized tissue were extracted with 5 times their volume by ethyl acetate and their supernatant were collected and evaporated to dryness. The process was repeated three times. The dry residues were dissolved in methanol and 25 μl of samples were injected in high-performance liquid chromatography (HPLC). JASCO HPLC systems (JASCO Corporations, Tokyo, Japan) with JASCO PU-2080 plus pump, JASCO UV-2075 plus detector, JASCO AS-2059 plus autosampler and Athena C-18 150 mm × 4.6 mm column (CNW Technologies) was used to evaluate the amount of quercetin at a wavelength of 354 nm. The mobile phase used was composed of water, methanol and acetonitrile (50:45:5, v/v) and the flow rate was maintained at 1 ml/min. Pharmacokinetic parameters were determined according to the concentration-time data. The area under the concentration-time curve (AUC) was analysed using linear trapezoidal rule. The elimination rate constant (K_e) was calculated from the slope of the concentration-time curve at the terminal phase and elimination half life ($t_{1/2}$) was calculated by dividing 0.693 by K_e.

TUNEL Assay

Tumor tissue was isolated, fixed in 2% paraformaldehyde, and embedded in optimal cutting temperature (OCT) compound. Subsequently, 7 μm of frozen sections were cut and TUNEL (terminal deoxynucleotidyl transferased UTP nick-end labeling) assay was performed using *In situ* apoptosis detection kit (Takara Bio. Inc., MK500, Japan), according to manufacturer's protocol. Briefly, the endogenous peroxidase was inactivated by methanol and permeabilisation buffer was added. Slides were then incubated for 1.5 h at 37°C in a humidified incubator with solution containing terminal deoxynucleotidyl transferase (TdT) enzyme. Tumor sections were further washed and incubated with antibody and stained with diaminobenzidine. Slides were examined under inverted microscope (Axio-observer.A1, Carl Zeiss, Germany) at 200× magnification to assess apoptotic cells with DNA fragmentation.

Statistical Analysis

To analyze the data statistically, Graphpad Prism 5.0 (San Diego, CA) software was used. Data was evaluated by two-tailed Student's *t*-test and value of $P<0.05$ was considered statistically significant.

RESULTS

Synthesis and Characterization of MPEG-PLA-Qu Nanoparticles

The schematic representation of MPEG-PLA-Qu nanoparticles synthesis is given in Fig. 1. The mean particle size of MPEG-PLA-Qu nanoparticles was analyzed by electrophoretic light scattering (ELS) study. Figure 2a indicates that the zeta average of freshly synthesized unloaded MPEG-PLA and quercetin loaded MPEG-PLA-Qu nanoparticles were 142.1 ±2.8 nm and 155.3±3.2 nm, respectively. The increase in size of MPEG-PLA-Qu nanoparticles may be attributed to the loaded quercetin [24]. The poly-dispersity index (PDI) of nanoparticle was 0.2±0.05 indicating narrow size distributions. Additionally, MPEG-PLA-Qu nanoparticles, synthesized here, showed a zeta potential of −3.14 mV (Fig. 2b) which was higher in comparison to previously reported PLA or PLGA nanoparticles having zeta potential of −50 mV [25].

The size and surface morphology of MPEG-PLA-Qu nanoparticles was interpreted by TEM and AFM images after diluting nanoparticle formulation with distilled water. A representative TEM image of quercetin loaded MPEG-PLA nanoparticles revealed that the nanoparticles were monodispersed and spherical in shape with size distribution ranging from 100 to 200 nm (Fig. 2c). AFM images reflected multilayer deposition of spherical nanoparticles with different height on silicon surface with average nanoparticle size of <150 nm (Fig. 2d). The particle size as observed by TEM and AFM is always less than that determined

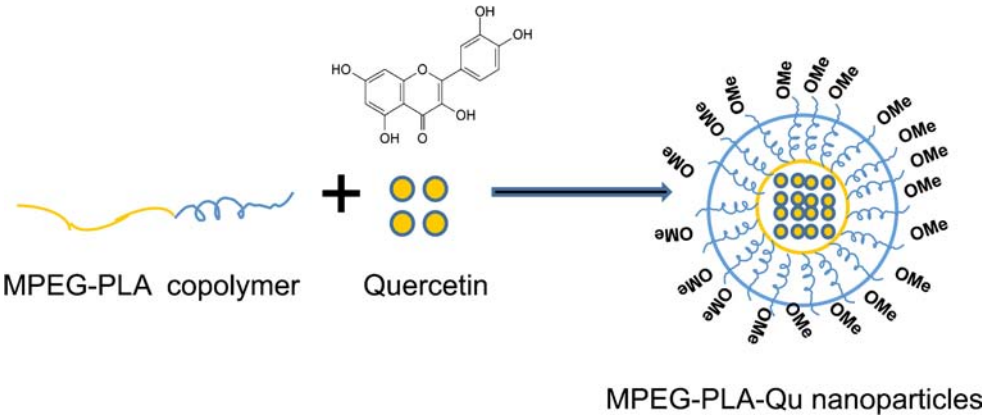

Fig. 1 Schematic diagram showing synthesis of MPEG-PLA-Qu nanoparticles.

by ELS because TEM and AFM interprets the size of dry particles while ELS analyzes hydrodynamic area because of the solvent effect. This phenomenon is due to the folding of PEG chain and aggregation of nanoparticles during the drying stage which mainly depends upon the thickness of the polymeric wall.

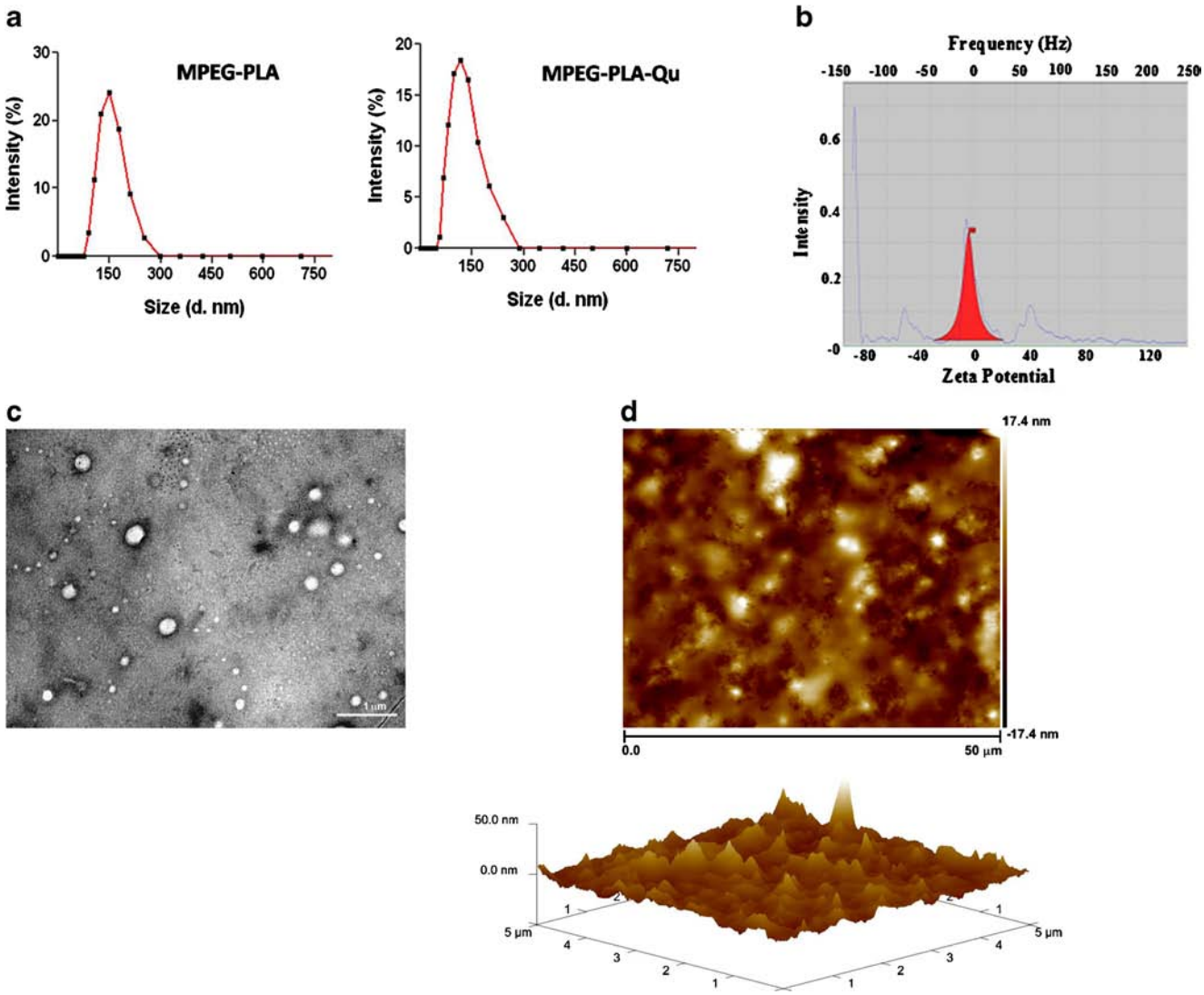

Fig. 2 Characterization of quercetin loaded MPEG-PLA nanoparticles. (**a**) Size of MPEG-PLA and quercetin loaded MPEG-PLA nanoparticles. (**b**) Zeta potential of MPEG-PLA-Qu nanoparticles. (**c**) TEM image of MPEG-PLA-Qu nanoparticles stained with 1% phosphotungstic acid. (d) AFM images of MPEG-PLA-Qu nanoparticles.

The synthesized MPEG-PLA nanoparticles were quantified for their drug loading percent and encapsulation efficiency by absorption spectra at 380 nm using calibration curve which was generated by known concentrations of quercetin solutions. The drug loading level of quercetin encapsulated in MPEG-PLA nanoparticles was 5.3 ± 1.1% and their quercetin encapsulation efficiency was 62.8 ± 2.9%. The physicochemical characterization of MPEG-PLA-Qu nanoparticles indicated their application as nano-drug delivery system.

In Vitro Drug Release Profile of Quercetin from MPEG-PLA-Qu Nanoparticles

As the size of MPEG-PLA-Qu nanoparticles were falling in 100–200 nm range, passive targeting of quercetin to tumor cells was expected. Therefore, the *in vitro* drug release pattern of MPEG-PLA-Qu nanoparticles at physiological pH 7.4 was studied to determine the long term sustained release pattern of drug from nanoparticles. During the initial 24 h, around 35% of quercetin was released from the nanoparticles. It is evident from the drug release pattern that MPEG-PLA-Qu nanoparticles showed bulk release during the first phase and slow release for prolonged time during the later phase (Fig. 3) [26].

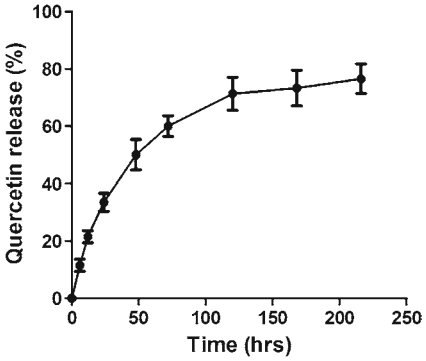

Fig. 3 *In vitro* release pattern of quercetin at pH 7.4. Similar results were obtained in three independent experiments. Data are shown as mean ± SD.

Anticancer Effect of MPEG-PLA-Qu Nanoparticles in MDA-MB-231 Breast Cancer Cell Line

The anticancer effect of quercetin encapsulated in MPEG-PLA nanoparticles in comparison to free quercetin was assessed by MTT and LDH assay. MDA-MB-231 cells incubated with different doses of MPEG-PLA-Qu nanoparticles showed decreased cell viability and increased cytotoxicity in a dose dependent manner. In detail, the cell viability of cells treated with free quercetin (13.5 μg/ml) and encapsulated quercetin (13.5 μg/ml) at 96 h was 34 and 38% lower than their respective control groups (Fig. 4a). In consistence to the cell viability assay, the cytotoxicity assay also showed that both free quercetin and encapsulated quercetin treatment groups, at 13.5 μg/ml dose, exhibited ~17% cytotoxicity to their respective control groups (Fig. 4b). However, blank MPEG-PLA nanoparticles did not show any prominent cytotoxic effect on cells indicating their nontoxic behavior at the tested concentration. These results indicate that, the cytotoxic effect of loaded quercetin onto MPEG-PLA-Qu nanoparticles was approximately equal to that of free quercetin at a similar dose (13.5 μg/ml) after 96 h of treatment.

Induction of Cell Apoptosis by MPEG-PLA-Qu Nanoparticles in MDA-MB-231 Cells

To determine the apoptotic effect of MPEG-PLA encapsulated quercetin in MDA-MB-231 cells, the cells were stained with Annexin V-FITC and PI, and analyzed using flow cytometry. Results showed dose dependent increase in the percentage of annexin V-FITC-positive and PI-positive cells (Fig. 4c). The apoptosis rate was 22.4, 29.8 and 31.1%, respectively when cells were treated with 3.375, 6.75 and 13.5 μg/ml of encapsulated quercetin for 72 h, as compared to blank MPEG-PLA nanoparticle treatment group (14.6%). Significant increase in the population of late apoptotic cells was observed with an increase in treatment doses.

Quantitative Measurement of Quercetin in Cell Lysate

Quantitative study was done to estimate the amount of quercetin level confined within the cell lysate after 72 h of treatment. Prominent differences in quercetin level were observed from MDA-MB-231 cells of each treatment groups (Fig. 5). Study showed dose-dependent increase in the amount of quercetin in the cells treated with encapsulated quercetin. In comparison to cells treated with encapsulated quercetin, less amount of quercetin level was detected in the cells treated with free querectin at the same dose (13.5 μg/ml).

Intracellular Uptake and Subcellular Localization of MPEG-PLA-Qu-NR Nanoparticles

The internalization of MPEG-PLA-Qu-NR by MDA-MB-231 cells was demonstrated by confocal microscopic images. Nuclei and endoplasmic reticulum (ER) were stained with DAPI (blue dye) and ER tracker (green dye), respectively. The localization of Nile Red in the cells can be detected by the presence of red fluorescence. Following treatment, the co-localization of MPEG-PLA-Qu-NR nanoparticles with ER was observed as yellow spots emerging due to overlapping green and red fluorescence (Fig. 6a). Confocal images of MPEG-PLA-Qu-NR nanoparticles treated cells, taken at predetermined time points, revealed that the uptake of nanoparticles by the cells initiated within 1 h of treatment which further exists inside the cells even after 72 h of treatment

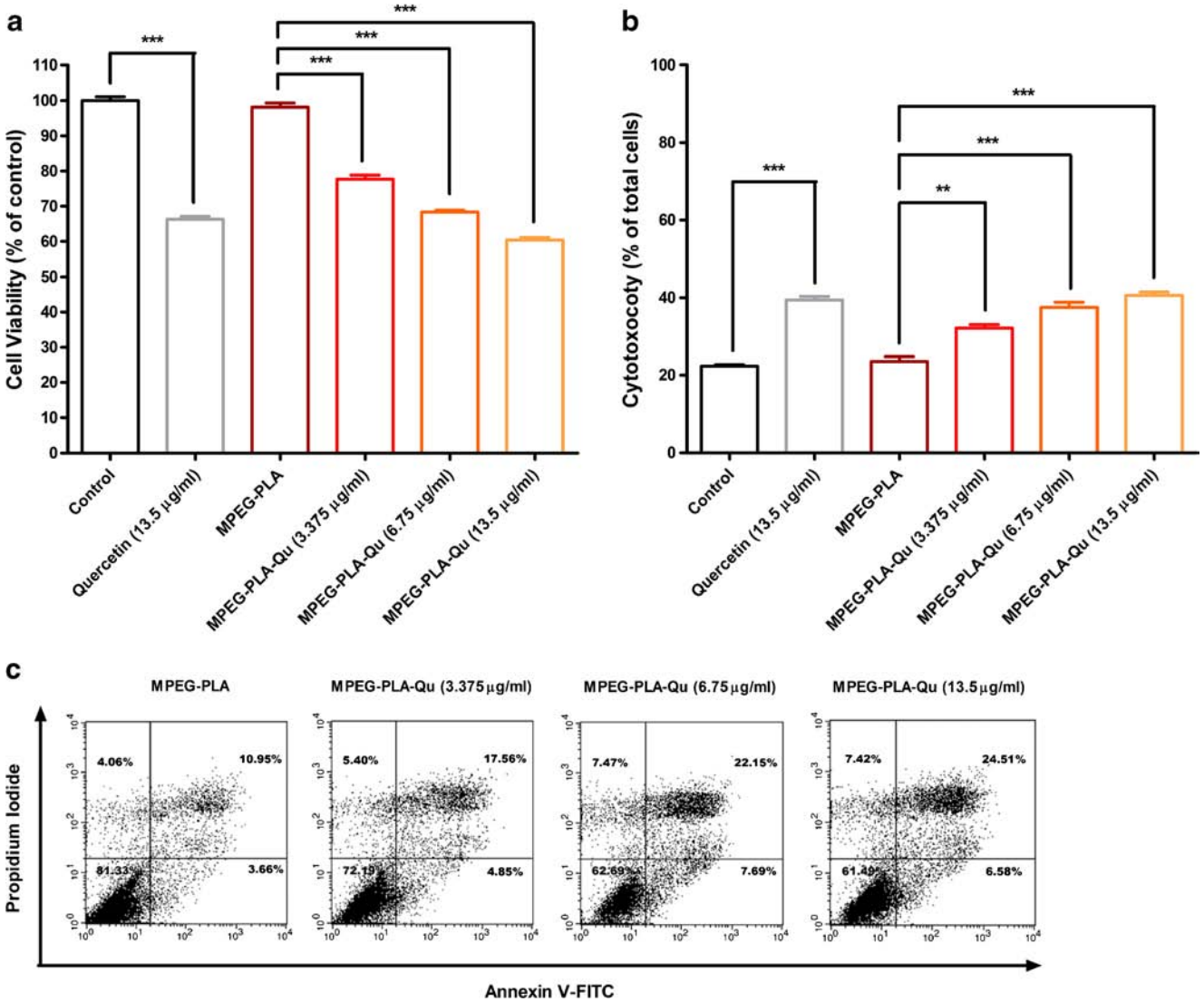

Fig. 4 Effect of free quercetin (13.5 μg/ml), MPEG-PLA-Qu (6.75 μg/ml equivalent to free quercetin) and MPEG-PLA-Qu (13.5 μg/ml equivalent to free quercetin) on viability and cytotoxicity of MDA-MB-231 cells after 96 h of treatment. (**a**) Cell viability was estimated by MTT assay. (**b**) Cell cytotoxicity was estimated by LDH assay. (**c**) Flow cytometric analysis of apoptotic MDA-MB-231 cells after 72 h of treatment with MPEG-PLA nanoparticles. Similar results were obtained in three independent experiments. Data are shown as mean ± SD. $^{*}p < 0.05$, $^{**}p < 0.01$, $^{***}p < 0.001$.

(Fig. 6b). On the contrary, the cells treated with native Nile Red showed red fluorescence on the outer surface of cells.

Antitumor Efficacy of MPEG-PLA-Qu Nanoparticles on Mouse Xenograft Model

To study the antitumor efficiency of MPEG-PLA-Qu nanoparticles on xenograft mice model developed by 4 T1 mammary cancer cells *in vivo*, tumor volume and tumor weight were observed after administrating free quercetin and encapsulated quercetin nanoparticles peritumorally (Fig. 7a and c, respectively). Female BALB/c mice were treated with MPEG-PLA-Qu nanoparticles at the doses of 0.5 and 4 mg/kg of loaded quercetin and free quercetin at the dose of 4 mg/kg, after the tumor volume reached 100–200 mm^3. In comparison to respective control groups, significant inhibition in tumor growth was observed by both free quercetin and MPEG-PLA encapsulated quercetin treatment groups, dose dependently. At 22 days post inoculation, the average tumor weight of free quercetin treated group was 81.4 mg as compared to encapsulated quercetin treated groups, *i.e.* 90.0 and 60.0 mg (respectively for 0.5 and 4 mg/kg treatment groups). These data indicate that MPEG-PLA encapsulated quercetin showed more reduction in tumor volume and weight as compared to free quercetin at similar dose. Furthermore, similar extent of tumor growth inhibition with free quercetin was obtained by nearly 8 fold less dose of encapsulated quercetin (0.5 mg/kg). During the study, the body weight of mice was almost constant in all the treatment groups, indicating that the drug and polymer treatment was well tolerated by the animals

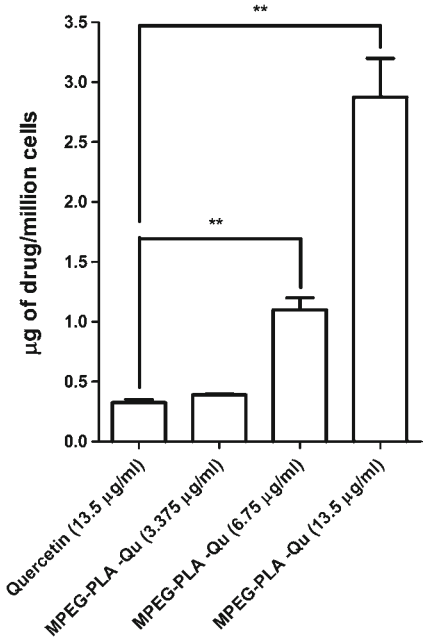

Fig. 5 Quantitative estimation of quercetin in cell lysate after 72 h of treatment. Similar results were obtained in three independent experiments. Data are shown as mean ± SD. *$p < 0.05$, **$p < 0.01$, ***$p < 0.001$.

(Fig. 7b). Fig. 7d shows representative tumors from each treatment groups.

Pharmacokinetics Following Peritumoral Injection of MPEG-PLA-Qu Nanoparticles

The quercetin level in tumor and plasma samples collected from mice injected with free quercetin and MPEG-PLA-Qu nanoparticles were compared at defined time points. Figure 7e depicts the biphasic mannered decline in quercetin retention level at the tumor site. There was a rapid decline in MPEG-PLA encapsulated quercetin concentration level (~40%) within 12 h of injection pointing towards the initial burst release of quercetin which further continued to gradually decline (~64%) until 72 h of injection due to slow release of quercetin from nanoformulations ($t_{1/2} = 43.32 \pm 3.3$). In comparison, tumors excised from mice with free quercetin treatment showed fast elimination of quercetin from tissue site to the detection limit within 72 h of treatment as apparent by the short half life of quercetin in tumor vicinity ($t_{1/2} = 16 \pm 2.4$). Significant increase in the concentration of encapsulated quercetin was detected at 72 h of MPEG-PLA-Qu treatment against free quercetin. Additionally, the area under the concentration-time curve (AUC_{0-t}) also increased in the tumors excised from MPEG-PLA-Qu treatment groups suggesting elongated retention of quercetin in the tumors (Table I). However, the difference in AUC between the treatment groups was not significant which may be due to large coefficients of variations. In contrast, the concentration of quercetin in plasma samples collected from both the treatment groups was under the detectable limit at all the time points (data not shown) which may be accredited to the peritumoral mode of injection [27].

Histological Analysis of Tumors for Apoptotic Study

Induction of apoptosis in MPEG-PLA-Qu treated tumor tissues was detected by TUNEL assay. Images of tumor section were taken near the surface of tumor tissue to show maximum apoptotic cells occurrence. The dark brown stained cells confirmed the fragmented nuclei in excised tumor sections (Fig. 8a). Significant increase in TUNEL positive apoptotic cells resulted from the treatment with MPEG-PLA-Qu nanoparticles in comparison to free quercetin treatment at a similar dose (4 mg/kg; Fig. 8b).

DISCUSSION

The systemic toxicity and reduced incursion of chemotherapeutic drugs into breast tissue is leading into constant demands for developing new therapeutic agents capable of eliminating these problems and are clinically applicable against breast cancer [28]. Plants are known to possess pharmacological diversified properties and are rich source of clinically important phytochemicals against various diseases, including cancer. Among them, quercetin is a well known flavonoid present in many natural herbs. It has been earlier associated with various pharmacological activities including anticancer activity against numerous cell types [29]. Here, to

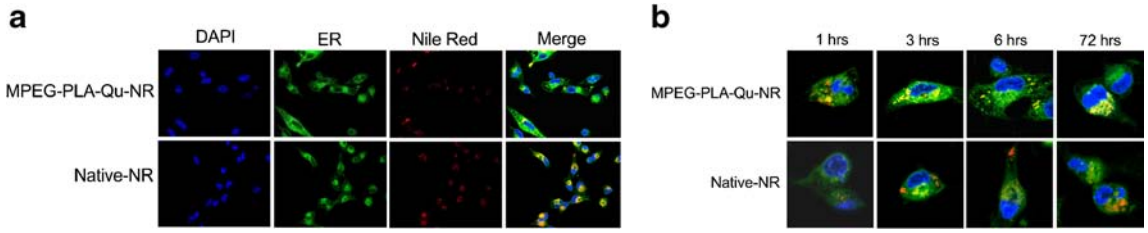

Fig. 6 Confocal microscopic images of free Nile Red and MPEG-PLA-Qu-NR nanoparticles (**a**) Images taken after 6 h of treatment and stained with ER tracker (green for endosplamic reticulum) and DAPI (blue for nucleus). Nile Red is represented by red colour. The overlapping signals of ER tracker and Nile Red are characterized by the presence of yellow colour spots. (**b**) Confocal images of MPEG-PLA-Qu-NR uptake process taken at 1, 3, 6 and 72 h of treatment, respectively.

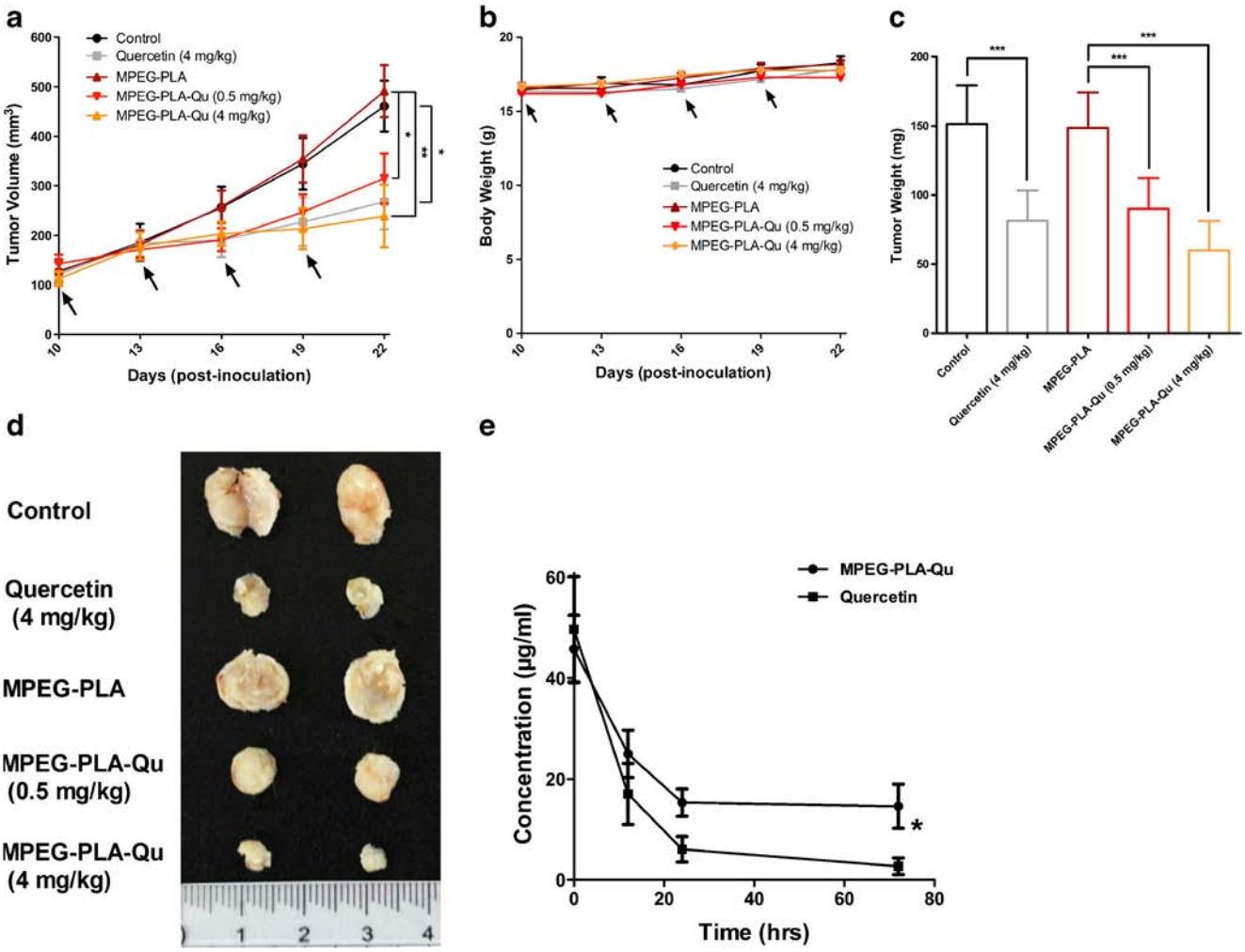

Fig. 7 *In vivo* antitumor efficacy of free quercetin and MPEG-PLA-Qu nanoparticles. (**a**) Tumor volume progression after repeated peritumoral treatments of free quercetin (4 mg/kg), MEG-PLA-Qu (0.5 mg/kg equivalent to free quercetin) and MPEG-PLA-Qu (4 mg/kg equivalent to free quercetin). (**b**) Body weight progression. (**c**) Tumor weight on 22nd day. (**d**) Representative photographs of excised tumors from each treatment group. (**e**) Quercetin concentration at tumor site after single peritumoral injection of free quercetin and MPEG-PLA-Qu (4 mg/kg equivalent to free quercetin). At specific time points (0, 12, 24, and 72 h), group of 5 mice were sacrificed and tumors were excised and analyzed for quercetin concentration using HPLC. Similar results were obtained in three independent experiments. Data are shown as mean ± SD. *$p < 0.05$, **$p < 0.01$, ***$p < 0.001$. Arrows indicate treatment time points.

overcome the restrictions associated with *in vivo* delivery of quercetin, MPEG-PLA copolymer was used to encapsulate quercetin for better water solubility (Fig. 1). The presence of hydrophilic MPEG minimizes the particle uptake by non targeted cells rendering protection from detecting by macrophages [15]. In addition, MPEG could provide an aqueous membrane outside of the nanoparticles which assists in holding back the release of hydrophobic drug for sustained release [30]. To reduce systemic toxicity and to increase drug concentration at the loco-regional site of major tumor load, peritumoral injection of MPEG-PLA encapsulated quercetin nanoparticles was employed.

Table I Tumor Pharmacokinetic Parameters of Peritumorally Injected Freeree Quercetin and MPEG-PLA-Qu Nanoparticles ($n = 5$)

Formulation	C_{last} (µg/ml)	T_{last} (h)	$t_{1/2}$ (h)	AUC_{0-72} (µg h/ml)
Quercetin	2.7 ± 1.6	72	16 ± 2.4	740.9 ± 149.6
MPEG-PLA-Qu np	14.6 ± 2.5*	72	43.32 ± 3.3**	1,385 ± 153.9

C_{last}, last measured concentration; T_{last}, last time at which concentration was measured; $t_{1/2}$, half life; *AUC*, area under curve. Data are shown as mean ± SD. *$p < 0.05$, **$p < 0.01$.

It has been suggested that the polymeric nanoparticles with an average diameter less than 200 nm are ideal for *in vivo* drug delivery [31]. Therefore, the selection of an optimal formulation in the study was based on the nanoparticle size (≤200 nm), which was confirmed by ELS analysis. Different nanoformulations were synthesized by varying components. Variables selected were different type of organic solvents and surfactants (Table S1). In order to synthesize MPEG-PLA-Qu nanoparticles, acetonitrile as an organic solvent and Pluronic F-68 as a surfactant were selected. The size distribution pattern of particles provides an insight to their drug release behavior and fate at cellular level and

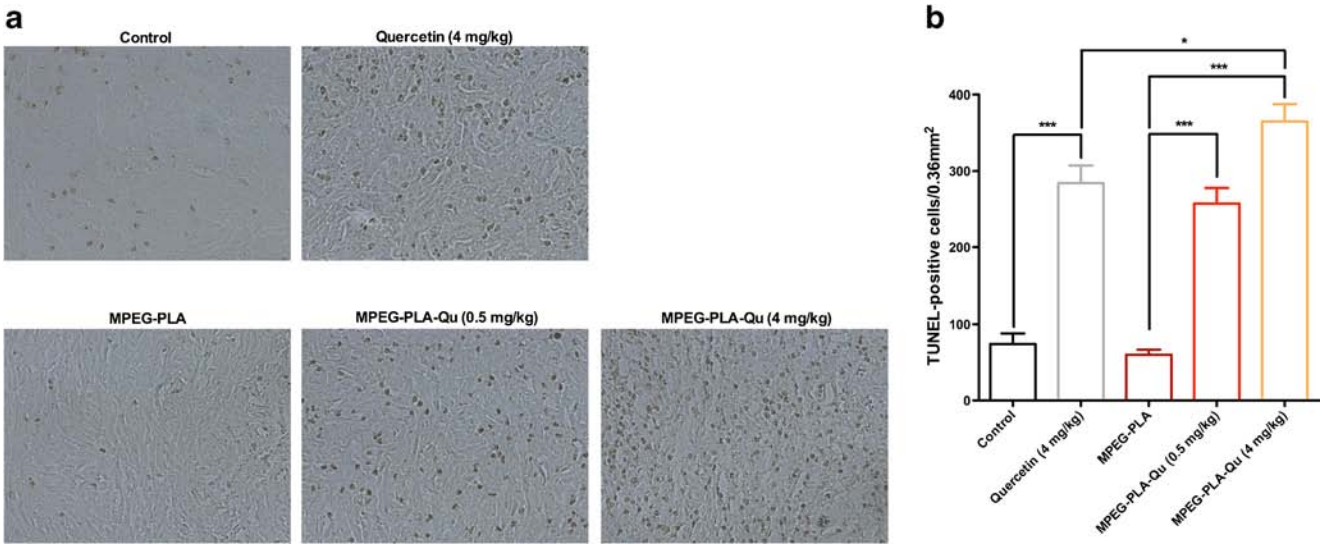

Fig. 8 Apoptotic cells as demonstrated by TUNEL assay in excised tumor sections. (**a**) Microscopic images of tumor sections. (**b**) Apoptosis frequencies in tumor sections treated with free quercetin and MPEG-PLA-Qu nanoparticles. Similar results were obtained in three independent experiments. Data are shown as mean ± SD. *$p < 0.05$, **$p < 0.01$, ***$p < 0.001$.

after *in vivo* administration [32]. Because of the smaller particle size (<200 nm) of MPEG-PLA-Qu nanoparticles (Fig. 2), they may be assumed to be compatible in enhanced permeability and retension (EPR) targeting attributed to the leaky nature of tumor vessels and may show increased accumulation at the tumor site. Moreover, less PDI (<0.4) of synthesized particles also reflects homogeneity of the nanosuspension [33]. Furthermore, the MPEG layer can shift the shear plane of the disperse layer to a greater distance from the nanospheres which can be indicated by zeta potential. In the present study the resulting zeta potential was −3.14 mV which can be considered sufficient to avoid RES recognition [34].

Previously, it has been reported that nanoparticles with less than 200 nm in size are internalized more efficiently inside the cells by clathrin-mediated endocytosis [35]. Thus, the drug release pattern was studied *in vitro* to predict the drug release behavior of MPEG-PLA-Qu nanoparticles *in vivo* (Fig. 3). The burst release of quercetin during initial phase can be attributed to the release and dissolution of quercetin present on the surface of nanoparticles, while slow release during later phase may be due to slow diffusion of quercetin from the polymeric matrix. The encapsulation of hydrophobic quercetin in a biodegradable polymer makes it difficult to permeate through the matrix rendering the sustained release property to the prepared MPEG-PLA-Qu nanoparticles. The rate of release of hydrophobic drug mainly depends upon the rate of the copolymeric nanoparticle degradation, interaction between drug and nanoparticle core, length of the core block, drug loading content *etc.* In this study, MPEG-PLA-Qu nanoparticles showed good sustained release of quercetin which may provides stable drug concentration after treatment facilitating continual and long term therapeutic effect.

The *in vitro* dose dependent cytotoxic activity of MPEG-PLA-Qu nanoparticles on MDA-MB-231 breast cancer cells was also demonstrated using MTT and LDH assay (Fig. 4). However, the cytotoxic effect of MPEG-PLA-Qu nanoparticles (13.5 μg/ml of loaded quercetin) was almost similar to that of free quercetin at the same concentration after 96 h of treatment. According to *in vitro* drug release assay, sustained release of quercetin from nanoparticles over a long period of time was already hypothesized. Therefore, it can be assumed that there was incomplete release of quercetin from nanoparticles after 96 h of treatment. Thus, prolonged cytotoxic effect of quercetin loaded nanoparticles can be expected even after 96 h of treatment. It is expected that MPEG-PLA encapsulated quercetin could possibly improve the anticancer effect of free quercetin which may be owed to either enhanced uptake of nanoparticles by cells or due to controlled release of quercetin from nanoparticles.

In accordance to *in vitro* drug release assay, querectin level in cells was quantified (Fig. 5). Jain *et al.* (2013) quantitatively demonstrated that in Caco-2 cells there was 6 fold increase in the concentration of quercetin encapsulated in PLGA polymer [36]. In consistence, our result also showed approximately 7 fold increase in the concentration of quercetin in encapsulated form compared to free quercetin in MDA-MB-231 breast cancer cells. Similarly, confocal microscopic images of Nile Red encapsulated MPEG-PLA-Qu-NR nanoparticles also showed high uptake and localization of nanoparticles within the treated cells (Fig. 6). Moreover, MPEG-PLA-Qu-NR nanoparticles were found co-localized with ER suggesting their role in inducing specific cellular responses, as previously reported by Paulo *et al.* [37]. Increased quercetin level might be due to high solubility of PEG in the cell membrane, facilitating cellular association and entry of encapsulated drug inside the cell [38]. Increased amount of quercetin level in MPEG-PLA-Qu treated cells indicates prolonged cytotoxic

effect by enhanced uptake or delayed release of quercetin from nanoparticles. Thus, inside the cells, the nanoparticles could play the role of drug storehouse, exerting their cytotoxic effect for a longer period of time in comparison to non-encapsulated drug. To explain the anticancer mechanism of quercetin, the apoptotic effects of MPEG-PLA-Qu nanoparticles on MDA-MB-231 breast cancer cells were also investigated. In consideration, apoptosis is known as the major mechanism by which most anticancer drugs act including quercetin [39]. Flow cytometry confirmed the dose dependent induction of apoptosis after 72 h of treatment with MPEG-PLA-Qu nanoparticles.

To determine the antitumor potential of MPEG-PLA-Qu nanoparticles, peritumoral mode of administration was selected as an alternative of targeted delivery to minimize the systemic toxicity and to increase the drug concentration at the site of action [40, 41]. For localized delivery the nanoparticles are administered subcutaneously or peritumorally from where they are taken up by regional lymph nodes [9]. Furthermore, lymphatic targeting is an advance of chemotherapy to cure lymphatic tumors or prevent metastases since nanoparticles can penetrate the interstitial space in the vicinity of injection site finally getting absorbed by the lymphatic capillaries into the lymphatic system. Moreover, peritumoral injection can also reduce the non-specific uptake of nanoparticles by other cellular systems. Here, free quercetin and MPEG-PLA-Qu nanoparticles were injected peritumorally in breast cancer BALB/c mice model. The results demonstrated that quercetin exhibited impressive *in vivo* antitumor activity without detectable toxicity in all the treatment groups which may be attributed to the peritumoral route of administration. Our data clearly indicate that MPEG-PLA encapsulated quercetin exhibits a similar extent of tumor growth inhibition at 8 folds fewer doses than free quercetin. Moreover, MPEG-PLA encapsulated quercetin also showed increased antitumor efficacy as compared to the same dose of free quercetin. This finding suggests that quercetin loaded MPEG-PLA nanoparticles possess better antitumor efficiency *in vivo* (Fig. 7), which may be owing to the sustained release of quercetin from nanoparticles as well as their better stability and high cellular uptake after being encapsulated by MPEG-PLA copolymer. Tumor pharmacokinetic experiments also confirmed that encapsulated quercetin was retained in tumor for extended time period as compared to free quercetin after peritumoral administration. Further, TUNEL assay showed dose-dependent increase in apoptotic cells frequency in tumor sections of encapsulated quercetin treatment group confirming the apoptotic mode of cell death (Fig. 8). Also, the apoptotic cells number was significantly raised in excised tumor from MPEG-PLA-Qu treatment groups compared to free quercetin treatment group. Thus, it can be suggested that peritumoral administration of MPEG-PLA-Qu nanoparticles could be used as an efficient drug delivery system.

In conclusion, this study demonstrated synthesis of quercetin loaded MPEG-PLA nanoparticles as a peritumoral delivery system that can efficiently prevent tumor growth progression and localization in an area. MPEG-PLA-Qu nanoparticles presented sustained release of quercetin and increased antitumor effect as compared to free quercetin. Our results clearly demonstrated that MPEG-PLA-Qu nanoparticles show anticancer activity by inducing apoptosis in MDA-MB-231 breast cancer cells and also implies the enhanced *in vivo* therapeutic efficiency of peritumorally administered MPEG-PLA encapsulated quercetin. However, further studies are needed to increase the therapeutic potential of MPEG-PLA-Qu nanoparticles to much higher extent by functionalizing them with targeting moieties or by combinatory encapsulation with other drugs. It will also be interesting to study the detailed apoptotic mechanism of MPEG-PLA-Qu nanoparticles to formulate more potent and effective anticancer drug.

ACKNOWLEDGEMENTS AND DISCLOSURES

This research was supported by Basic Science Research Program through the National Research Foundation of Korea (NRF) funded by the Ministry of Education (2011-001-4792), by a grant of the Korea Health Technology R&D Project through the Korea Health Industry Development Institute (KHIDI), funded by the Ministry of Health &Welfare, Republic of Korea (HI12C1265), and by Hallym University Research Fund.

REFERENCES

1. World Health Organization. International agency for research on cancer (IARC). GLOBOCAN 2012: estimated incidence, mortality and prevalence worldwide in 2012; 2014 February. Available from: http://globocan.iarc.fr (under Fact Sheets, choose "Breast" and "World").
2. Terao J, Piskula M, Yao Q. Protective effect of epicatechin, epicatechin gallate, and quercetin on lipid peroxidation in phospholipid bilayers. Arch Biochem Biophys. 1994;308:278–84.
3. Heijnen CG, Haenen GR, van Acker FA, van der Vijgh WJ, Bast A. Flavonoids as peroxynitrite scavengers: the role of the hydroxyl groups. Toxicol in Vitro. 2001;15:3–6.
4. Formica JV, Regelson W. Review of the biology of Quercetin and related bioflavonoids. Food Chem Toxicol. 1995;33:1061–80.
5. Park MH. Min do S. Quercetin-induced downregulation of phospholipase D1 inhibits proliferation and invasion in U87 glioma cells. Biochem Biophys Res Commun. 2011;412:710–5.
6. Zheng SY, Li Y, Jiang D, Zhao J, Ge JF. Anticancer effect and apoptosis induction by quercetin in the human lung cancer cell line A-549. Mol Med Rep. 2012;5:822–6.
7. Passamonti S, Terdoslavich M, Franca R, Vanzo A, Tramer F, Braidot E, *et al.* Bioavailability of flavonoids: a review of their membrane transport and the function of bilitranslocase in animal and plant organisms. Curr Drug Metab. 2009;10:369–94.

8. Puoci F, Morelli C, Cirillo G, Curcio M, Parisi OI, Maris P, *et al.* Anticancer activity of a quercetin-based polymer towards HeLa cancer cells. Anticancer Res. 2012;32:2843–7.
9. Gabizon AA. Stealth liposomes and tumor targeting: one step further in the quest for the magic bullet. Clin Cancer Res. 2001;7:223–5.
10. Kumari A, Yadav SK, Yadav SC. Biodegradable polymeric nanoparticles based drug delivery systems. Colloids Surf B: Biointerfaces. 2010;75:1–18.
11. Kumari A, Kumar V, Yadav SK. Plant extract synthesized PLA nanoparticles for controlled and sustained release of quercetin: a green approach. PLoS One. 2012;7:e41230.
12. Nie S, Xing Y, Kim GJ, Simons JW. Nanotechnology applications in cancer. Annu Rev Biomed Eng. 2007;9:257–88.
13. Kim K, Yu M, Zong X, Chiu J, Fang D, Seo YS, *et al.* Control of degradation rate and hydrophilicity in electrospun non-woven poly(D, L-lactide) nanofiber scaffolds for biomedical applications. Biomaterials. 2003;24:4977–85.
14. Danhier F, Feron O, Preat V. To exploit the tumor microenvironment: passive and active tumor targeting of nanocarriers for anticancer drug delivery. J Control Release. 2010;148:135–46.
15. Owens 3rd DE, Peppas NA. Opsonization, biodistribution, and pharmacokinetics of polymeric nanoparticles. Int J Pharm. 2006;307:93–102.
16. Kobayashi H, Kawamoto S, Sakai Y, Choyke PL, Star RA, Brechbiel MW, *et al.* Lymphatic drainage imaging of breast cancer in mice by micro-magnetic resonance lymphangiography using a nano-size paramagnetic contrast agent. J Natl Cancer Inst. 2004;96:703–8.
17. Hagiwara A, Takahashi T, Sawai K, Sakakura C, Shirasu M, Ohgaki M, *et al.* Selective drug delivery to peri-tumoral region and regional lymphatics by local injection of aclarubicin adsorbed on activated carbon particles in patients with breast cancer–a pilot study. Anti Cancer Drugs. 1997;8:666–70.
18. Gao X, Wang B, Wei X, Men K, Zheng F, Zhou Y, *et al.* Anticancer effect and mechanism of polymer micelle-encapsulated quercetin on ovarian cancer. Nanoscale. 2012;4:7021–30.
19. Farokhzad OC, Cheng J, Teply BA, Sherifi I, Jon S, Kantoff PW, *et al.* Targeted nanoparticle-aptamer bioconjugates for cancer chemotherapy *in vivo*. Proc Natl Acad Sci U S A. 2006;103:6315–20.
20. Yin P, Wang Y, Qiu Y, Hou L, Liu X, Qin J, *et al.* Bufalin-loaded mPEG-PLGA-PLL-cRGD nanoparticles: preparation, cellular uptake, tissue distribution, and anticancer activity. Int J Nanomedicine. 2012;7:3961–9.
21. Khoee S, Rahmatolahzadeh R. Synthesis and characterization of pH-responsive and folated nanoparticles based on self-assembled brush-like PLGA/PEG/AEMA copolymer with targeted cancer therapy properties: a comprehensive kinetic study. Eur J Med Chem. 2012;50:416–27.
22. Kunwar A, Barik A, Mishra B, Rathinasamy K, Pandey R, Priyadarsini KI. Quantitative cellular uptake, localization and cytotoxicity of curcumin in normal and tumor cells. Biochim Biophys Acta. 2008;1780:673–9.
23. Demaria S, Kawashima N, Yang AM, Devitt ML, Babb JS, Allison JP, *et al.* Immune-mediated inhibition of metastases after treatment with local radiation and CTLA-4 blockade in a mouse model of breast cancer. Clin Cancer Res. 2005;11:728–34.
24. Kumari A, Yadav SK, Pakade YB, Kumar V, Singh B, Chaudhary A, *et al.* Nanoencapsulation and characterization of Albizia chinensis isolated antioxidant quercitrin on PLA nanoparticles. Colloids Surf B: Biointerfaces. 2011;82:224–32.
25. Govender T, Stolnik S, Garnett MC, Illum L, Davis SS. PLGA nanoparticles prepared by nanoprecipitation: drug loading and release studies of a water soluble drug. J Control Release. 1999;57:171–85.
26. Shuai X, Ai H, Nasongkla N, Kim S, Gao J. Micellar carriers based on block copolymers of poly(epsilon-caprolactone) and poly(ethylene glycol) for doxorubicin delivery. J Control Release. 2004;98:415–26.
27. Samlowski WE, Mc Gregor JR, Jurek M, Baudys M, Zentner GM, Fowers KD. ReGel polymer-based delivery of interleukin-2 as a cancer treatment. J Immunother. 2006;29:524–35.
28. Chen JH, Ling R, Yao Q, Li Y, Chen T, Wang Z, *et al.* Effect of small-sized liposomal Adriamycin administered by various routes on a metastatic breast cancer model. Endocr Relat Cancer. 2005;12:93–100.
29. Corvazier E, Maclouf J. Interference of some flavonoids and nonsteroidal anti-inflammatory drugs with oxidative metabolism of arachidonic acid by human platelets and neutrophils. Biochim Biophys Acta. 1985;835:315–21.
30. Pan G, Lemmouchi Y, Akala EO, Bakare O. Studies on PEGylated and Drug-Loaded PAMAM Dendrimers. J Bioact Compat Polym. 2005;20:113–28.
31. Lamprecht A, Schafer U, Lehr CM. Size-dependent bioadhesion of micro- and nanoparticulate carriers to the inflamed colonic mucosa. Pharm Res. 2001;18:788–93.
32. Potineni A, Lynn DM, Langer R, Amiji MM. Poly(ethylene oxide)-modified poly(beta-amino ester) nanoparticles as a pH-sensitive biodegradable system for paclitaxel delivery. J Control Release. 2003;86:223–34.
33. Chitkara D, Nikalaje S, Mittal A, Chand M, Kumar N. Development of quercetin nanoformulation and *in vivo* evaluation using streptozotocin induced diabetic rat model. Drug Deliv Transl Res. 2012;2:112–23.
34. Gref R, Domb A, Quellec P, Blunk T, Müller RH, Verbavatz JM, *et al.* The controlled intravenous delivery of drugs using PEG-coated sterically stabilized nanospheres. Advanced drug delivery reviews. Suppl. 2012;64:316–26.
35. Rejman J, Oberle V, Zuhorn IS, Hoekstra D. Size-dependent internalization of particles *via* the pathways of clathrin- and caveolae-mediated endocytosis. Biochem J. 2004;377(Pt 1):159–69.
36. Jain AK, Thanki K, Jain S. Co-encapsulation of tamoxifen and quercetin in polymeric nanoparticles: implications on oral bioavailability, antitumor efficacy, and drug-induced toxicity. Mol Pharm. 2013;10:3459–74.
37. Paulo CS, Pires das Neves R, Ferreira LS. Nanoparticles for intracellular-targeted drug delivery. Nanotechnology. 2011;22:494002–12.
38. Yamazaki M, Ito T. Deformation and instability of membrane structure of phospholipid vesicles caused by osmophobic association: mechanical stress model for the mechanism of poly(ethylene glycol)-induced membrane fusion. Biochemistry. 1990;29:1309–14.
39. Kim H, Seo EM, Sharma AR, Ganbold B, Park J, Sharma G, *et al.* Regulation of Wnt signaling activity for growth suppression induced by quercetin in 4 T1 murine mammary cancer cells. Int J Oncol. 2013;43:1319–25.
40. Parveen S, Sahoo SK. Nanomedicine: clinical applications of polyethylene glycol conjugated proteins and drugs. Clin Pharmacokinet. 2006;45:965–88.
41. Sahoo SK, Ma W, Labhasetwar V. Efficacy of transferrin-conjugated paclitaxel-loaded nanoparticles in a murine model of prostate cancer. Int J Cancer. 2004;112:335–40.